

# Robust MMSE Precoding and Power Allocation for Cell-Free Networks

Victoria M. T. Palhares, Andre R. Flores and Rodrigo C. de Lamare

<sup>1</sup> Centre for Telecommunications Studies, Pontifical Catholic University of Rio de Janeiro, Brazil

<sup>2</sup> Department of Electronic Engineering, University of York, United Kingdom

Emails: victoriapalhares@cetuc.puc-rio.br, andre.flores@cetuc.puc-rio.br, delamare@cetuc.puc-rio.br.

**Abstract**—We consider the downlink of a cell-free massive multiple-input multiple-output (MIMO) system with single-antenna access points (APs) and single-antenna users. An iterative robust minimum mean-square error (RMMSE) precoder based on generalized loading is developed to mitigate interference in the presence of imperfect channel state information (CSI). An achievable rate analysis is carried out and optimal and uniform power allocation schemes are developed based on the signal-to-interference-plus-noise ratio. An analysis of the computational costs of the proposed RMMSE and existing schemes is also presented. Numerical results show the improvement provided by the proposed RMMSE precoder against linear minimum mean-square error, zero-forcing and conjugate beamforming precoders in the presence of imperfect CSI.

**Index Terms**—Cell-free massive MIMO, robust MMSE precoding, power allocation, distributed antenna systems.

## I. INTRODUCTION

Cell-free massive multiple-input multiple-output (MIMO) systems have emerged in recent years as a combination of massive MIMO, distributed antenna systems (DAS) and network MIMO [1], [2], where many randomly distributed access points (APs) are connected to a central processing unit (CPU) and serve simultaneously a much smaller number of users. At the CPU, precoding and power allocation algorithms are performed. Cell-free concepts have been shown to increase energy efficiency (EE) and per-user throughput over cellular systems in rural and urban scenarios [3], [4], [5]. Moreover, they can have simple signal processing thanks to favorable propagation with channel hardening [3]. Precoding is a key interference mitigation technique [6], [7], [8], [9], [10], [11], [12], [13], [14], [15], [16], [17], [18], [19], [20], [21], [22], [23], [24], [25] for the downlink of wireless networks, which has been considered for cell-free networks [4], [5], [26], [27]. Low-complexity conjugate beamforming (CB) has been investigated in [4]. Zero-forcing (ZF) precoding has been studied in the context of EE maximization in [5]. CB and ZF precoding have been considered with power allocation to provide uniformly good service for all users in [26]. Scalable cell-free solutions with decentralized processing and clustering methods have been recently proposed to decrease the computational complexity of previous techniques and facilitate their deployment [28]. A minimum mean-square error (MMSE) combiner with both centralized and decentralized

implementation is presented in [29]. In [30], two distributed precoding methods were introduced, one called local partial ZF and local protective partial ZF. A clustering method based on a user-centric approach has been proposed so that users are served only by a subset of APs [31].

A key problem with transmit processing techniques for cell-free systems is how to deal with imperfect channel state information (CSI), which can significantly degrade the system performance. CSI is obtained by users sending known pilot sequences to the APs, which estimate the channel coefficients based on the received signal. The error is caused by noise, time-varying characteristics of the channel, which makes the obtained CSI outdated, pilot contamination and frequency offset. In practical systems, perfect CSI is impossible to be obtained, which calls for robust design techniques that can deal with imperfect CSI. Most precoders proposed in the literature consider perfect CSI, providing unrealistic solutions to practical scenarios. Therefore, the development of robust precoders that can deal with imperfect CSI is of great interest.

Robust techniques have been developed in sensor array signal processing to mitigate the effects of uncertainties. Although never applied to cell-free before, robust techniques can improve the performance of precoding and power allocation without increasing significantly the computational complexity. In particular, robust techniques include diagonal loading (DL) [32], [33], [34], generalized loading [35], worst-case optimization [36], [37], [38], [39], [40], [41] and subspace techniques [42]. Recently, robust techniques have been proposed for multiple-antenna systems. In [43], a robust precoder with per-antenna power constraint was considered, where the probability of outage of the signal-to-interference-plus-noise ratio (SINR) targets is minimized with imperfect CSI located at the base stations. Another robust precoder was developed in [44] using the ZF criterion and user grouping, with imperfect CSI at the receivers.

Robust precoders based on MMSE designs have been examined in [39], [37], [34], [45], [40], [41]. Worst-case optimization has been considered in [39] by minimizing the maximum mean-square error (MSE), taking into consideration the channel estimation matrix and the channel estimation error matrix. Reformulating the problem into a min-min convex minimization problem enables the solution to be found in closed form. Similarly, in [40], [41], the same objective function is used, with a tolerance for the channel estimation error, yet with total power constraint.

In this context, robust techniques have the potential to mitigate the effects of imperfect CSI in cell-free networks, which are particularly sensitive to the accuracy of CSI. Therefore, the motivation of this work is to develop a robust precoder suitable for cell-free networks. In particular, we develop an iterative robust MMSE (RMMSE) precoder based on generalized loading along with power allocation. A robust precoder is calculated based on initial parameters, used in power allocation and recalculated based on the power allocation coefficients. MMSE channel estimates are considered, similarly to previous works [26]. Additionally, optimal and uniform power allocation techniques are devised and compared with existing CB, ZF and MMSE precoding and power allocation techniques [26], [4] in terms of bit error rate (BER), sum-rate, and per-user rate, taking into account imperfect CSI. Moreover, analytical expressions are derived to compute the sum rates of the proposed approaches and their computational costs are evaluated.

We propose a novel iterative RMMSE precoder for a cell-free massive MIMO system scenario, which not only minimizes the mean-square error (MSE) but also has the ability to minimize the effect of channel estimation errors. The iterative RMMSE precoder introduces a generalized loading technique, where a regularization factor containing the statistics of the channel estimation error matrix is added to the MSE objective function. We also present an optimal and uniform power allocation strategy directly related to the maximization of the minimum SINR, considering the proposed RMMSE precoder. Moreover, we present a computational complexity analysis of the proposed and existing techniques, which shows that they are comparable in terms of computational cost. Numerical results demonstrate that the proposed RMMSE precoder with UPA and OPA have an improved performance compared to previous methods in terms of BER, sum-rate and per-user rate.

The rest of this paper is organized as follows. In Section II the cell-free massive MIMO system model and CSI scenarios are detailed. In Section III, an iterative RMMSE precoder with power allocation is presented. An analysis of the sum rates and the computational costs are considered in Section IV. In Section V, numerical results and discussions are presented, whereas in Section VI conclusions are drawn.

*Notation:* Uppercase bold symbols denote matrices and lowercase bold symbols denote vectors. The superscripts  $()^*$ ,  $()^T$ ,  $()^H$  stand for complex conjugate, transpose and Hermitian operations, respectively. The expectation, trace of a matrix, real part of the argument, Euclidean norm and Frobenius norm are denoted by  $\mathbb{E}[\cdot]$ ,  $\text{tr}(\cdot)$ ,  $\text{Re}(\cdot)$ ,  $\|\cdot\|_2$  and  $\|\cdot\|_F$ , respectively. The operator  $\text{diag}\{\mathbf{V}\}$  retains the main diagonal elements of  $\mathbf{V}$  in a column vector. The  $D \times D$  identity matrix is  $\mathbf{I}_D$  and the  $D \times E$  zero matrix is  $\mathbf{0}_{D \times E}$ .  $x \sim \mathcal{N}(0, \sigma^2)$  refers to a Gaussian random variable (RV)  $x$  with zero mean and variance  $\sigma^2$  and  $x \sim \mathcal{CN}(0, \sigma^2)$  denotes a circularly symmetric complex Gaussian RV  $x$  with zero mean and variance  $\sigma^2$ .

## II. SYSTEM MODEL

The downlink of a cell-free massive MIMO system is considered with  $M$  randomly distributed single-antenna APs

and  $U$  single-antenna users, where  $M \gg U$ . In this system, all APs are connected to a CPU and serve simultaneously all users, as shown in Fig. 1.

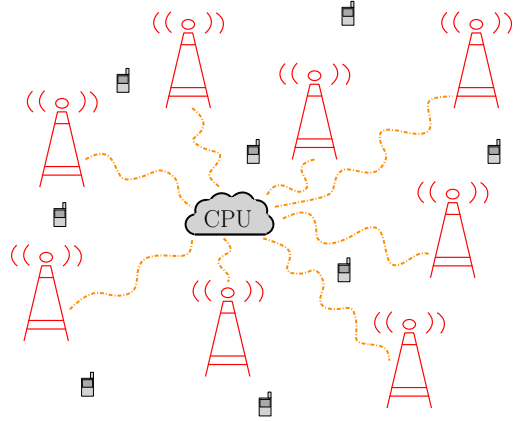


Fig. 1. Cell-free massive MIMO system.

The channel coefficient between the  $m$ th AP and the  $u$ th user is defined as [4]

$$g_{m,u} = \sqrt{\beta_{m,u}} h_{m,u}, \quad (1)$$

where  $\beta_{m,u}$  is the large-scale fading coefficient (due to path loss and shadowing effects) and  $h_{m,u} \sim \mathcal{CN}(0, 1)$  is the small-scale fading coefficient, defined as independent and identically distributed (i.i.d) RVs that remain constant during a coherence interval and are independent in different coherence intervals. The large-scale fading coefficients change less frequently, being constant for several coherence intervals. In this case, we assume that they change at least 40 times slower than  $h_{m,u}$  [4] and that pilot contamination is negligible [26].

The system employs the time division duplex (TDD) protocol, which relies on the reciprocity principle to acquire the CSI at the transmitter. Then, the CSI is sent to the CPU, which performs precoding and power allocation to reduce the multi-user interference. By considering MMSE estimates of CSI at each AP, we define them as [26]

$$\hat{g}_{m,u} \sim \mathcal{CN}(0, \alpha_{m,u}), \quad \tilde{g}_{m,u} \sim \mathcal{CN}(0, \beta_{m,u} - \alpha_{m,u}), \quad (2)$$

where  $\hat{g}_{m,u}$  is the CSI estimate between the  $m$ th AP and the  $u$ th user and  $\tilde{g}_{m,u}$  is the CSI error between the  $m$ th AP and the  $u$ th user. To evaluate different levels of imperfect CSI, we consider  $\alpha_{m,u}$  as an adjustable percentage of  $\beta_{m,u}$  ( $0 \leq \alpha_{m,u} \leq 1$ ). Thus, we have

$$\begin{aligned} \alpha_{m,u} &= n\beta_{m,u} \\ \tilde{g}_{m,u} &= g_{m,u} - \hat{g}_{m,u}, \quad \text{and} \\ \mathbb{E}[|\tilde{g}_{m,u}|^2] &= (1-n)\beta_{m,u}. \end{aligned} \quad (3)$$

## III. PROPOSED RMMSE PRECODING AND POWER ALLOCATION

In this section, a fully digital RMMSE precoder is derived and two power allocation techniques are introduced. We then present an algorithm which iteratively combines the precoding and power control solutions.

### A. Proposed RMMSE Precoder

In the downlink of a cell-free setting with precoding and power allocation, the signal received by the  $u$ th user is

$$y_u = \sqrt{\rho_f} \mathbf{g}_u^T \mathbf{P} \mathbf{N} \mathbf{s} + w_u, \quad (4)$$

where  $\rho_f$  is the maximum transmit power of each AP,  $\mathbf{g}_u = [g_{1,u}, \dots, g_{M,u}]^T$  are the channel coefficients for user  $u$ ,  $\mathbf{P} \in \mathbb{C}^{M \times U}$  is the precoding matrix,  $\mathbf{N} \in \mathbb{R}_+^{U \times U}$  is the power allocation diagonal matrix with  $\sqrt{\eta_1}, \dots, \sqrt{\eta_U}$  on its diagonal,  $\eta_u$  is the power coefficient of user  $u$ ,  $\mathbf{s} = [s_1, \dots, s_U]^T$  is the zero mean symbol vector, with  $\sigma_s^2 = \mathbb{E}(|s_u|^2)$ ,  $s_u$  is the data symbol intended for user  $u$ , which is uncorrelated among users,  $w_u \sim \mathcal{CN}(0, \sigma_w^2)$  is the additive noise for user  $u$  and  $\sigma_w^2$  is the noise variance. Similar to [4], [26],  $\mathbf{N}$  weights the symbols intended for each user,  $s_u$ , by a factor  $\sqrt{\eta_u}$ , where  $u = 1, \dots, U$ . We compute  $\mathbf{P}$  and  $\mathbf{N}$  in an alternating fashion to solve the precoding and power allocation problems. The combined signal with all users is described by

$$\begin{aligned} \mathbf{y} &= \sqrt{\rho_f} \mathbf{G}^T \mathbf{P} \mathbf{N} \mathbf{s} + \mathbf{w} \\ &= \sqrt{\rho_f} \left( \hat{\mathbf{G}} + \tilde{\mathbf{G}} \right)^T \mathbf{P} \mathbf{N} \mathbf{s} + \mathbf{w} \\ &= \sqrt{\rho_f} \hat{\mathbf{G}}^T \mathbf{P} \mathbf{N} \mathbf{s} + \underbrace{\sqrt{\rho_f} \tilde{\mathbf{G}}^T \mathbf{P} \mathbf{N} \mathbf{s}}_{\Delta} + \mathbf{w} \end{aligned} \quad (5)$$

where  $\mathbf{G} \in \mathbb{C}^{M \times U}$  is the channel matrix, which varies according to an ergodic stationary process,  $\hat{\mathbf{G}} \in \mathbb{C}^{M \times U}$  is the CSI matrix,  $\tilde{\mathbf{G}} \in \mathbb{C}^{M \times U}$  is the CSI error matrix and  $\mathbf{w} = [w_1, \dots, w_U]^T$  is the noise vector.

The design of the proposed RMMSE precoder has two main objectives: to minimize the MSE under a total power constraint and to mitigate the effects of CSI errors,  $\mathbb{E}[\|\Delta\|_2^2] \rightarrow 0$ . Therefore, we add a regularization term multiplied by the scalar  $\Gamma$  to adjust the regularization effects. The proposed RMMSE precoder solves the following optimization:

$$\{\mathbf{P}_{\text{RMMSE}}, \mathbf{N}, f_{\text{RMMSE}}\} = \underset{\{\mathbf{P}, \mathbf{N}, f\}}{\text{argmin}} \mathbb{E} \left[ \|\mathbf{s} - f^{-1} \mathbf{y}\|_2^2 \right] + \Gamma \text{tr} \left( \mathbf{M} \mathbf{P} \mathbf{N} \mathbf{C}_s \mathbf{N}^H \mathbf{P}^H \right) \quad (6a)$$

$$\text{subject to } \mathbb{E}[\|\mathbf{x}\|_2^2] = E_{\text{tr}} \quad (6b)$$

where  $f^{-1}$  is a normalization factor at the receivers, which can be interpreted as an automatic gain control [46], and the transmit signal is given by

$$\mathbf{x} = \sqrt{\rho_f} \mathbf{P} \mathbf{N} \mathbf{s}. \quad (7)$$

The average transmit power is described by

$$\mathbb{E}[\|\mathbf{x}\|_2^2] = \rho_f \text{tr} \left( \mathbf{P} \mathbf{N} \mathbf{C}_s \mathbf{N}^H \mathbf{P}^H \right) = E_{\text{tr}}, \quad (8)$$

where  $\mathbf{C}_s = \mathbb{E}[\mathbf{s} \mathbf{s}^H]$  is the symbol covariance matrix.

The regularization factor contains the auxiliary matrix

$$\mathbf{M} = \theta \mathbb{E} \left[ \tilde{\mathbf{G}}^* \tilde{\mathbf{G}}^T \right], \quad (9)$$

where  $\mathbb{E}[\tilde{\mathbf{G}}^* \tilde{\mathbf{G}}^T]$  is a diagonal matrix with  $\sum_{u=1}^U ((1-n)\beta_{m,u})$  on its  $m$ th diagonal element and  $\theta$  is a chosen scalar. Although  $\mathbf{M}$  is diagonal, the diagonal

elements are not equal. The proposed regularization is categorized as a generalized loading [35], where the matrix is usually obtained through steering vector errors and complemented by a scalar. Here, we employ a matrix  $\mathbf{M}$  obtained from the statistics of the CSI error matrix  $\tilde{\mathbf{G}}$  and scaled by a constant  $\theta$  as an adaptation of the technique to the design of robust MMSE precoding for cell-free networks.

By constructing the Lagrangian function with the Lagrange multiplier,  $\lambda$ , setting its derivatives to zero and considering a power allocation matrix  $\mathbf{N}$ , we can compute the precoder  $\mathbf{P}$  and the normalization  $f$ , as shown below:

$$\begin{aligned} \mathcal{L}(\mathbf{P}, \mathbf{N}, f, \Gamma, \lambda) &= \mathbb{E} \left[ \|\mathbf{s} - f^{-1} \mathbf{y}\|_2^2 \right] + \Gamma \text{tr} \left( \mathbf{M} \mathbf{P} \mathbf{N} \mathbf{C}_s \mathbf{N}^H \mathbf{P}^H \right) \\ &+ \lambda \left( \rho_f \text{tr} \left( \mathbf{P} \mathbf{N} \mathbf{C}_s \mathbf{N}^H \mathbf{P}^H \right) - E_{\text{tr}} \right) \\ &= \text{tr}(\mathbf{C}_s) - f^{-1} \sqrt{\rho_f} \text{tr} \left( \hat{\mathbf{G}}^T \mathbf{P} \mathbf{N} \mathbf{C}_s \right) - f^{-1} \sqrt{\rho_f} \text{tr} \left( \hat{\mathbf{G}}^* \mathbf{C}_s \mathbf{N}^H \mathbf{P}^H \right) \\ &+ f^{-2} \rho_f \text{tr} \left( \hat{\mathbf{G}}^* \hat{\mathbf{G}}^T \mathbf{P} \mathbf{N} \mathbf{C}_s \mathbf{N}^H \mathbf{P}^H \right) + f^{-2} \text{tr}(\mathbf{C}_w) + \Gamma \text{tr} \left( \mathbf{M} \mathbf{P} \mathbf{N} \mathbf{C}_s \mathbf{N}^H \mathbf{P}^H \right) \\ &+ \lambda \left( \rho_f \text{tr} \left( \mathbf{P} \mathbf{N} \mathbf{C}_s \mathbf{N}^H \mathbf{P}^H \right) - E_{\text{tr}} \right), \end{aligned} \quad (10)$$

where  $\mathbf{C}_w = \mathbb{E}[\mathbf{w} \mathbf{w}^H]$  is the noise covariance matrix.

Using the result of the partial derivative,  $\partial \text{tr}(\mathbf{B} \mathbf{X}^H) / \partial \mathbf{X}^* = \mathbf{B}$ , we obtain the following expressions:

$$\begin{aligned} \frac{\partial \mathcal{L}(\mathbf{P}, \mathbf{N}, f, \Gamma, \lambda)}{\partial \mathbf{P}^*} &= -f^{-1} \sqrt{\rho_f} \hat{\mathbf{G}}^* \mathbf{C}_s \mathbf{N}^H + f^{-2} \rho_f \hat{\mathbf{G}}^* \hat{\mathbf{G}}^T \mathbf{P} \mathbf{N} \\ &\mathbf{C}_s \mathbf{N}^H + \Gamma \mathbf{M} \mathbf{P} \mathbf{N} \mathbf{C}_s \mathbf{N}^H + \lambda \rho_f \mathbf{P} \mathbf{N} \mathbf{C}_s \mathbf{N}^H = 0, \end{aligned} \quad (11)$$

and

$$\begin{aligned} \frac{\partial \mathcal{L}(\mathbf{P}, \mathbf{N}, f, \Gamma, \lambda)}{\partial f} &= f^{-2} \sqrt{\rho_f} \text{tr} \left( \hat{\mathbf{G}}^T \mathbf{P} \mathbf{N} \mathbf{C}_s \right) + f^{-2} \sqrt{\rho_f} \text{tr} \left( \hat{\mathbf{G}}^* \mathbf{C}_s \mathbf{N}^H \mathbf{P}^H \right) \\ &- 2f^{-3} \rho_f \text{tr} \left( \hat{\mathbf{G}}^* \hat{\mathbf{G}}^T \mathbf{P} \mathbf{N} \mathbf{C}_s \mathbf{N}^H \mathbf{P}^H \right) - 2f^{-3} \text{tr}(\mathbf{C}_w) = 0. \end{aligned} \quad (12)$$

Solving for (11), we obtain

$$\mathbf{P} = \frac{f}{\sqrt{\rho_f}} \underbrace{\left( \hat{\mathbf{G}}^* \hat{\mathbf{G}}^T + \frac{\Gamma f^2}{\rho_f} \mathbf{M} + \lambda f^2 \mathbf{I}_M \right)^{-1}}_{\tilde{\mathbf{P}}} \hat{\mathbf{G}}^* \mathbf{N}^{-1} \quad (13)$$

By using the expression in (12), we arrive at

$$f \sqrt{\rho_f} \text{tr} \left( \hat{\mathbf{G}}^* \mathbf{C}_s \mathbf{N}^H \mathbf{P}^H \right) = \rho_f \text{tr} \left( \hat{\mathbf{G}}^* \hat{\mathbf{G}}^T \mathbf{P} \mathbf{N} \mathbf{C}_s \mathbf{N}^H \mathbf{P}^H \right) + \text{tr}(\mathbf{C}_w) \quad (14)$$

Using (11), we have

$$f \sqrt{\rho_f} \hat{\mathbf{G}}^* \mathbf{C}_s \mathbf{N}^H = \rho_f \hat{\mathbf{G}}^* \hat{\mathbf{G}}^T \mathbf{P} \mathbf{N} \mathbf{C}_s \mathbf{N}^H + \Gamma f^2 \mathbf{M} \mathbf{P} \mathbf{N} \mathbf{C}_s \mathbf{N}^H + \lambda f^2 \rho_f \mathbf{P} \mathbf{N} \mathbf{C}_s \mathbf{N}^H. \quad (15)$$

Pre-multiplying on the right by  $\mathbf{P}^H$  in (15), using the trace operator and considering  $\epsilon = \lambda f^2$ , the expression takes the form

$$\begin{aligned} f \sqrt{\rho_f} \text{tr} \left( \hat{\mathbf{G}}^* \mathbf{C}_s \mathbf{N}^H \mathbf{P}^H \right) &= \rho_f \text{tr} \left( \hat{\mathbf{G}}^* \hat{\mathbf{G}}^T \mathbf{P} \mathbf{N} \mathbf{C}_s \mathbf{N}^H \mathbf{P}^H \right) \\ &+ \Gamma f^2 \text{tr} \left( \mathbf{M} \mathbf{P} \mathbf{N} \mathbf{C}_s \mathbf{N}^H \mathbf{P}^H \right) + \epsilon \rho_f \text{tr} \left( \mathbf{P} \mathbf{N} \mathbf{C}_s \mathbf{N}^H \mathbf{P}^H \right). \end{aligned} \quad (16)$$

Equating expressions (14) and (16), we have

$$\begin{aligned}\text{tr}(\mathbf{C}_w) &= \Gamma f^2 \text{tr}(\mathbf{M}\mathbf{P}\mathbf{N}\mathbf{C}_s\mathbf{N}^H\mathbf{P}^H) + \epsilon \rho_f \text{tr}(\mathbf{P}\mathbf{N}\mathbf{C}_s\mathbf{N}^H\mathbf{P}^H) \\ \text{tr}(\mathbf{C}_w) &= \Gamma f^2 \text{tr}(\mathbf{M}\tilde{\mathbf{P}}\mathbf{N}\mathbf{C}_s\mathbf{N}^H\tilde{\mathbf{P}}^H) + \epsilon E_{tr}.\end{aligned}\quad (17)$$

By manipulating the expression, we obtain

$$\epsilon = \frac{\text{tr}(\mathbf{C}_w)}{E_{tr}} - \frac{\Gamma f_{\text{RMMSE}}^4 \text{tr}(\mathbf{M}\tilde{\mathbf{P}}\mathbf{C}_s\tilde{\mathbf{P}}^H)}{\rho_f E_{tr}} \quad (18)$$

where

$$f_{\text{RMMSE}} = \sqrt{(E_{tr}) / (\text{tr}(\tilde{\mathbf{P}}\mathbf{C}_s\tilde{\mathbf{P}}^H))}. \quad (19)$$

Therefore, the RMMSE precoder that takes into account power allocation for cell-free networks is given by

$$\begin{aligned}\mathbf{P}_{\text{RMMSE}} &= \frac{f_{\text{RMMSE}}}{\sqrt{\rho_f}} \left( \hat{\mathbf{G}}^* \hat{\mathbf{G}}^T + \frac{\text{tr}(\mathbf{C}_w)}{E_{tr}} \mathbf{I}_M \right. \\ &\quad \left. + \frac{\Gamma f_{\text{RMMSE}}^2 (E_{tr} \mathbf{M} - f_{\text{RMMSE}}^2 \text{tr}(\mathbf{M}\tilde{\mathbf{P}}\mathbf{C}_s\tilde{\mathbf{P}}^H) \mathbf{I}_M)}{\rho_f E_{tr}} \right)^{-1} \\ \hat{\mathbf{G}}^* \mathbf{N}^{-1} &= \frac{f_{\text{RMMSE}}}{\sqrt{\rho_f}} \tilde{\mathbf{P}} \mathbf{N}^{-1}.\end{aligned}\quad (20)$$

where  $\text{tr}(\mathbf{C}_w) = U\sigma_w^2$ . Note that if we assume perfect CSI, the error matrix  $\tilde{\mathbf{G}}$  goes to zero, i. e.,  $\hat{\mathbf{G}} = \mathbf{0}_{M \times U}$  and the RMMSE precoder becomes the MMSE precoder for cell-free networks. The same effect occurs if we set  $\Gamma = 0$ . Thus, the advantages of the RMMSE precoder will be only perceived in an imperfect CSI scenario.

## B. Power Allocation

In this section, we introduce Optimal Power Allocation (OPA) and Uniform Power Allocation (UPA) techniques applied to the RMMSE precoder. The objective is to find the power allocation matrix  $\mathbf{N}$ , a diagonal matrix with  $\sqrt{\eta_1}, \dots, \sqrt{\eta_U}$  on its main diagonal, which will be used to recompute the robust precoding matrix  $\mathbf{P}_{\text{RMMSE}}$  and the final power allocation matrix  $\mathbf{N}_{\text{RMMSE}}$ .

1) *Optimal Power Allocation (OPA)*: The chosen power allocation technique is optimal in terms of ensuring fairness among all users. The main point of this approach is to improve the performance of the user with the lowest SINR, meaning that all users will have at least a certain quality of service (QoS). The max-min fairness power allocation problem with AP power constraint for the RMMSE precoder can be formulated as

$$\max_{\boldsymbol{\eta}} \min_u \text{SINR}_u(\boldsymbol{\eta}) \quad (21a)$$

$$\text{s.t.} \sum_{i=1}^U \eta_i \delta_{m,i} \leq 1, m = 1, \dots, M, \quad (21b)$$

where  $\text{SINR}_u(\boldsymbol{\eta})$  denotes the SINR of user  $u$  as a function of  $\boldsymbol{\eta}$  and can be expressed as

$$\text{SINR}_u(\boldsymbol{\eta}) = \frac{\mathbb{E}[|C_1(\boldsymbol{\eta})|^2]}{\left(\sigma_w^2 + \sum_{i=1, i \neq u}^U \mathbb{E}[|C_{2,i}(\boldsymbol{\eta})|^2] + \mathbb{E}[|C_3(\boldsymbol{\eta})|^2]\right)}. \quad (22)$$

The term  $C_1(\boldsymbol{\eta})$  is the desired signal,  $\sigma_w^2$  is the noise variance,  $C_{2,i}(\boldsymbol{\eta})$  is the interference caused by user  $i$  for  $i \neq u, i = 1, \dots, U$ ,  $C_3(\boldsymbol{\eta})$  is the CSI error,  $\boldsymbol{\delta}_m = \text{diag}\{\mathbb{E}[\mathbf{p}_m^T \mathbf{p}_m^*]\}$ ,  $m = 1, \dots, M$ ,  $\mathbf{p}_m = [p_{m,1}, \dots, p_{m,U}]$  is the  $m$ th row of the precoder  $\mathbf{P}_{\text{RMMSE}}$  and  $\delta_{m,i}$  is the  $i$ th element of vector  $\boldsymbol{\delta}_m$ .

The power allocation problem can be expressed in an epigraph form as [4], [26], [47]

$$\text{find } \boldsymbol{\eta} \quad (23a)$$

$$\text{s.t. } \text{SINR}_u(\boldsymbol{\eta}) \geq t, u = 1, \dots, U, \quad (23b)$$

$$\sum_{i=1}^U \eta_i \delta_{m,i} \leq 1, m = 1, \dots, M, \quad (23c)$$

where  $t = \frac{t_b + t_e}{2}$  is the midpoint of a chosen interval  $(t_b, t_e)$ .

The problem in (24) is solved by addressing one feasibility problem at each step. First we assume that the problem is feasible. We set up the interval,  $[t_b, t_e]$  known to contain the optimal value  $t^*$ . Next, the convex feasibility problem is solved at its midpoint  $t = \frac{t_b + t_e}{2}$ , to decide whether the problem is feasible or not. If the problem is feasible, the upper interval is chosen, meaning that  $t_b = t$ . If, however, the problem is infeasible, the lower interval will now be evaluated, translating to  $t_e = t$ . The new interval will be half of the previous and the algorithm will be repeated until the resulting interval is smaller than a certain tolerance  $\epsilon$ ,  $|t_e - t_b| < \epsilon$ , [47].

2) *Uniform Power Allocation (UPA)*: We also present an alternative to the OPA scheme, based on [26]. In scenarios where a certain AP  $m$  transmits with full power and all  $\eta_u$ , for  $u = 1, \dots, U$  are equal, we have

$$\eta_u = 1 / \left( \max_m \sum_{i=1}^U \delta_{m,i} \right), u = 1, \dots, U, \quad (24)$$

where  $\delta_{m,i}$  is the  $i$ th element of vector  $\boldsymbol{\delta}_m$ . Although (24) is a suboptimal solution, it is less complex and a cost-effective alternative to show the benefits of the RMMSE precoder. Next, in Algorithm 1 we show how to combine the RMMSE precoder with power allocation. Each of the loops performs two iterations such that  $\text{ITER}_{\text{prec}} = \text{ITER}_{\text{pa}} = 2$ .

We initialize the algorithm with the precoding and power allocation matrix  $\tilde{\mathbf{P}}_{\text{MMSE}}$  and  $\mathbf{N}_{\text{MMSE}}$  obtained through the MMSE criterion with  $\Gamma = 0$ . After the MMSE precoder is obtained, we recursively calculate our initial  $f_{\text{RMMSE}}$  and  $\tilde{\mathbf{P}}$ , described in (19) and (20), respectively. Then, we enter the power allocation loop, where in the first iteration,  $\mathbf{P}_{\text{RMMSE}}$  is calculated considering  $\mathbf{N}[1] = \mathbf{N}_{\text{MMSE}}$ . The subsequent step is to find a new power allocation matrix  $\mathbf{N}$  based on the calculated precoder,  $\mathbf{P}_{\text{RMMSE}}$ . Then, the next precoding matrix will be computed with the new  $\mathbf{N}$ . The final step of the loop is to recalculate  $\mathbf{N}$  with the last RMMSE precoder found. Note that the final power allocation matrix  $\mathbf{N}_{\text{RMMSE}}$  satisfies

the power constraints and is different from the intermediate  $\mathbf{N}$  present in the precoding expression. Therefore they will not cancel each other. The scalar  $\theta$  is set as -1 to ensure that the diagonal elements of  $\mathbf{F}$  are always positive. Then  $\Gamma$  is chosen to maximize the SINR of the system.

---

**Algorithm 1** Proposed Iterative RMMSE Precoding
 

---

- 1: Find  $f_{\text{MMSE}}$ ,  $\tilde{\mathbf{P}}_{\text{MMSE}}$  and  $\mathbf{N}_{\text{MMSE}}$ , by considering  $\Gamma = 0$
  - 2: Initialize  $f_{\text{RMMSE}}[1] = f_{\text{MMSE}}$ ,  $\tilde{\mathbf{P}}[1] = \tilde{\mathbf{P}}_{\text{MMSE}}$ ,  $\theta = -1$ ,  $\mathbf{N}[1] = \mathbf{N}_{\text{MMSE}}$ ,  $\text{ITER}_{\text{prec}}$  (number of iterations for the precoder),  $\text{ITER}_{\text{pa}}$  (number of iterations for power allocation).
  - 3: **For**  $i=1:\text{ITER}_{\text{prec}}$   
 Update  $\Gamma$ ,  $\tilde{\mathbf{P}}$  and  $f_{\text{RMMSE}}$ :
  - 4: Calculate  $\Gamma[i+1]$  to optimize the SINR.
  - 5: Calculate  $\tilde{\mathbf{P}}[i+1] \leftarrow (20)$
  - 6: Calculate  $f_{\text{RMMSE}}[i+1] \leftarrow (19)$
  - 7: **end for**
  - 8: Obtain  $\tilde{\mathbf{P}} = \tilde{\mathbf{P}}[i+1]$  and  $f_{\text{RMMSE}} = f_{\text{RMMSE}}[i+1]$
  - 9: **For**  $j=1:\text{ITER}_{\text{pa}}$
  - 10: Calculate  $\mathbf{P}_{\text{RMMSE}}[j] \leftarrow (20)$
  - 11: Calculate  $\mathbf{N}[j+1] \leftarrow (23)$  or  $(24)$  (with fixed  $\mathbf{P}_{\text{RMMSE}}[j]$ )
  - 12: **end for**
  - 13: Obtain  $\mathbf{P}_{\text{RMMSE}} = \mathbf{P}_{\text{RMMSE}}[j]$  and  $\mathbf{N}_{\text{RMMSE}} = \mathbf{N}[j+1]$ .
- 

#### IV. SUM-RATE AND COMPLEXITY ANALYSIS

In this section, we present a sum-rate analysis of the proposed techniques along with the computational complexity of the proposed and existing algorithms.

##### A. Sum-Rate

Expanding expression (4), we obtain:

$$\begin{aligned}
 y_u &= \sqrt{\rho_f} \mathbf{g}_u^T \mathbf{P}_{\text{RMMSE}} \mathbf{N}_{\text{RMMSE}} \mathbf{s} + w_u \\
 &= \underbrace{\sqrt{\rho_f} \hat{\mathbf{g}}_u^T \mathbf{P}_{\text{RMMSE}} \mathbf{N}_{\text{RMMSE}} \mathbf{s}}_{\text{desired signal + interference}} + \underbrace{\sqrt{\rho_f} \tilde{\mathbf{g}}_u^T \mathbf{P}_{\text{RMMSE}} \mathbf{N}_{\text{RMMSE}} \mathbf{s}}_{\text{CSI error}} \\
 &\quad + w_u,
 \end{aligned} \tag{25}$$

where  $\hat{\mathbf{g}}_u = [\hat{g}_{1,u}, \dots, \hat{g}_{M,u}]^T$  is the CSI vector for user  $u$  and  $\tilde{\mathbf{g}}_u = [\tilde{g}_{1,u}, \dots, \tilde{g}_{M,u}]^T$  is the CSI error vector for user  $u$ .

Assuming Gaussian signalling, and based on the worst-case uncorrelated additive noise, the achievable rate of the  $u$ th user with the iterative RMMSE precoder is equal to [4], [26]

$$R_{u,\text{RMMSE}} = \log_2(1 + \text{SINR}_{u,\text{RMMSE}}). \tag{26}$$

The sum-rate expression is given by  $R_{\text{RMMSE}} = \sum_{u=1}^U R_{u,\text{RMMSE}}$ . The  $\text{SINR}_{u,\text{RMMSE}}$  is described by

$$\text{SINR}_{u,\text{RMMSE}} = \frac{\rho_f \eta_u \psi_u}{\sigma_w^2 + \rho_f \sum_{i=1, i \neq u}^U \eta_i \phi_{u,i} + \rho_f \sum_{i=1}^U \eta_i \gamma_{u,i}}, \tag{27}$$

where  $\psi_u = \mathbf{p}_u^H \hat{\mathbf{g}}_u^* \hat{\mathbf{g}}_u^T \mathbf{p}_u$ ,  $\phi_{u,i} = \mathbf{p}_i^H \hat{\mathbf{g}}_u^* \hat{\mathbf{g}}_u^T \mathbf{p}_i$ ,  $i \neq u$ ,  $i = 1, \dots, U$ ,  $\mathbf{p}_u = [p_{1,u}, \dots, p_{M,u}]^T$  is the column  $u$  of matrix  $\mathbf{P}_{\text{RMMSE}}$ ,  $\gamma_u = \text{diag}\{\mathbf{P}_{\text{RMMSE}}^H \mathbb{E}[\tilde{\mathbf{g}}_u^* \tilde{\mathbf{g}}_u^T] \mathbf{P}_{\text{RMMSE}}\}$ ,  $\gamma_{u,i}$  is the

$i$ th element of vector  $\gamma_u$ , and  $\mathbb{E}[\tilde{\mathbf{g}}_u^* \tilde{\mathbf{g}}_u^T]$  is a diagonal matrix with  $((1-n)\beta_{m,u})$  on its  $m$ th diagonal element.

To arrive at (27), we assumed that the symbols, noise and channel coefficients are mutually independent. With fading, the ergodic rate is taken by the expectation over all channel realizations, which can be obtained through a rate average, considering that sufficiently long codewords are transmitted. Since in  $\text{SINR}_{u,\text{RMMSE}}(\boldsymbol{\eta})$  the numerator and denominator are linear functions of  $\boldsymbol{\eta}$ , the expression is a quasilinear function, enabling us to use the bisection method [47].

##### B. Computational Complexity

We evaluate in this section the computational complexity of the proposed and existing methods. As shown in Table I, the complexity of the RMMSE precoder is comparable to the MMSE precoder (when  $\Gamma = 0$ ) and the ZF precoder from [26]. The CB precoder [4], [26] has inferior performance and much lower computational complexity as compared to the RMMSE, MMSE and ZF precoders. If  $M^3 > T_{\text{OPA}} U^{3.5}$ , the computational cost of RMMSE, MMSE and ZF with OPA will be  $\mathcal{O}(M^3)$ . Depending on the number of iterations of the bisection method,  $T_{\text{OPA}}$ , the OPA scheme may prevail when applied to all precoders. In contrast, if UPA is applied, it will not affect the complexity of the RMMSE, MMSE and ZF techniques. We conclude that the proposed RMMSE precoder has comparable computational cost to previous methods but can outperform existing precoders in the presence of imperfect CSI, as shown in Section V.

TABLE I  
COMPUTATIONAL COMPLEXITY

Precoding + Power Allocation	RMMSE Precoder	$\mathcal{O}(M^3)$
	MMSE Precoder	$\mathcal{O}(M^3)$
	ZF Precoder	$\mathcal{O}(M^3)$
	CB Precoder [4], [26]	$\mathcal{O}(MU)$
SINR Computation	RMSE Precoder	$\mathcal{O}(M^2 U^2)$
	MMSE Precoder	$\mathcal{O}(M^2 U^2)$
	ZF Precoder	$\mathcal{O}(M^2 U^2)$
	CB Precoder	$\mathcal{O}(MU^2)$
Power Allocation	OPA	$\mathcal{O}(T_{\text{OPA}} U^{3.5})$
	UPA	$\mathcal{O}(MU^2)$

#### V. NUMERICAL RESULTS

In this section, we compare the RMMSE precoder to the CB and ZF precoders and most importantly, to the MMSE scheme. Note that all simulations consider imperfect CSI since under perfect CSI the RMMSE precoder converges to the MMSE precoder for cell-free. In all experiments, we performed 500 channel realizations and assumed  $\sigma_s^2 = 1$ .

We consider the APs and users to be uniformly distributed within an area of 1 km<sup>2</sup>. The large-scale fading coefficients from (1) are modeled by

$$\beta_{m,u} = \Upsilon_{m,u} \cdot 10^{\frac{\sigma_{sh} z_{m,u}}{10}}, \tag{28}$$

where  $\Upsilon$  is the path loss and  $10^{\frac{\sigma_{sh} z_{m,u}}{10}}$  refers to the shadow fading with standard deviation  $\sigma_{sh} = 8$  dB and  $z_{m,u} \sim$

$\mathcal{N}(0, 1)$ . The path loss is based on a three-slope model [48], in dB, defined as

$$\Upsilon_{m,u} = \begin{cases} -L - 35 \log_{10}(d_{m,u}), & \text{if } d_{m,u} > d_1 \\ -L - 15 \log_{10}(d_1) - 20 \log_{10}(d_{m,u}), & \text{if } d_0 < d_{m,u} \leq d_1 \\ -L - 15 \log_{10}(d_1) - 20 \log_{10}(d_0), & \text{if } d_{m,u} \leq d_0 \end{cases} \quad (29)$$

where

$$L \triangleq 46.3 + 33.9 \log_{10}(\varrho) - 13.82 \log_{10}(h_{\text{AP}}) - (1.1 \log_{10}(\varrho) - 0.7) h_u + (1.56 \log_{10}(\varrho) - 0.8), \quad (30)$$

$d_{m,u}$  is the distance between the  $m$ th AP and the  $u$ th user,  $d_1 = 50$  m,  $d_0 = 10$  m,  $\varrho = 1900$  MHz is the carrier frequency in MHz,  $h_{\text{AP}} = 15$  m is the AP antenna height in meters and  $h_u = 1.65$  m is the user antenna height in meters, as in [4]. When  $d_{m,u} \leq d_1$  there is no shadowing.

We consider strong path loss, which is typical of cell-free systems, and define the signal-to-noise ratio (SNR) as

$$\text{SNR} = \frac{\rho_f \mathbb{E}[\|\hat{\mathbf{G}}\|_F^2]}{\text{tr}(\mathbf{C}_w)} = \frac{\rho_f \text{tr}(\hat{\mathbf{G}}\hat{\mathbf{G}}^H)}{U\sigma_w^2}, \quad (31)$$

where  $\sigma_w^2 = T_0 \times k_B \times B \times NF(W)$ ,  $T_0 = 290$  (Kelvin) is the noise temperature,  $k_B = 1.381 \times 10^{-23}$  (Joule per Kelvin) is the Boltzmann constant,  $B = 20$  MHz is the bandwidth and  $NF = 9$  dB is the noise figure. In (31), we fix  $\mathbf{C}_w$  and  $\hat{\mathbf{G}}$  and vary  $\rho_f$  according to the change in SNR values, which will be made throughout the experiments.

In the first example, shown in Fig. 2, we compare the strategies in terms of BER vs. SNR with UPA and OPA. We assume imperfect CSI with  $n = 0.99$  (1%), quadrature phase shift keying (QPSK) modulation and packets with 100 symbols (or 200 bits). This scenario assumes  $M = 96$  single-antenna APs and  $U = 8$  users.

The gains of the RMMSE precoder are substantial over the MMSE precoder of [46]. In addition, RMMSE with OPA can outperform MMSE with OPA and ZF with UPA by up to 3 dB and 4.6, respectively, at BER = 0.02. Note that the RMMSE precoder with OPA attains a consistent gain between 1.1 and 1.7 dB when compared to UPA, up to SNR = 20 dB.

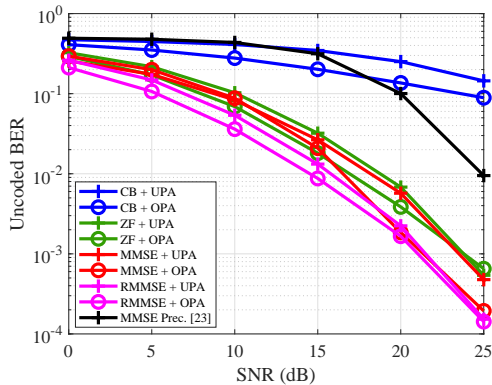


Fig. 2. BER vs. SNR with  $M = 96$ ,  $U = 8$ ,  $n = 0.99$ , 500 channel realizations, 100 symbols per packet,  $E_{tr} = M\rho_f$ .

In Table II we assess the BER of different precoding schemes at SNR = 25 dB. To this end, we vary the level of CSI imperfection, by modifying  $n$ , while the other parameters

TABLE II  
BER WITH UPA AT SNR = 25 dB

	$n = 0.99$	$n = 0.95$	$n = 0.9$
RMMSE	$1.25 \times 10^{-4}$	$3.49 \times 10^{-4}$	$1.6 \times 10^{-3}$
MMSE	$3.64 \times 10^{-4}$	$1.1 \times 10^{-3}$	$3.4 \times 10^{-3}$
ZF	$4.3 \times 10^{-4}$	$1.2 \times 10^{-3}$	$3.5 \times 10^{-3}$

remain the same as in the first example.

Notice that for  $n = 0.99$  the difference between the BER of the RMMSE and the MMSE precoder is  $2.39 \times 10^{-4}$ . When  $n$  is reduced to 95%, the gap is increased to  $7.56 \times 10^{-4}$ . For  $n = 0.9$ , the BER of the RMMSE precoder has a difference of  $1.8 \times 10^{-3}$ , compared to that from the MMSE precoder.

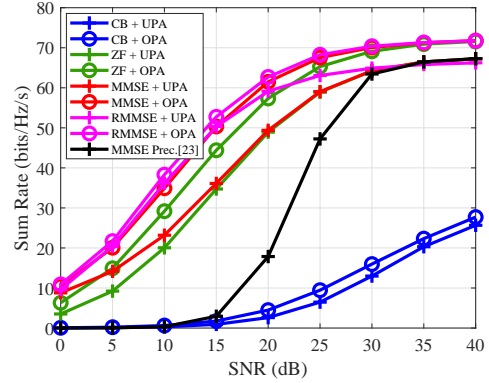


Fig. 3. Sum-rate vs. SNR with  $M = 128$ ,  $U = 16$ ,  $n = 0.9$ , 500 channel realizations and  $E_{tr} = M\rho_f$ .

The last experiment compares the analyzed techniques in terms of sum-rate vs. SNR and cumulative distribution function (CDF) vs. per-user rate with  $n = 0.9$  (10%). Moreover, we enlarge the system and employ  $M = 128$  single-antenna APs, and  $U = 16$  users. In Fig. 3, when OPA is used with precoding, all rates are improved as compared to UPA. For the RMMSE precoder the use of OPA instead of UPA results in a gain of 13% at SNR = 0 dB. Significant gains are also obtained for the RMMSE precoder with OPA over MMSE with UPA, which is around 65% at SNR = 10 dB, and for RMMSE with OPA over ZF with OPA, which can be up to 72%.

In terms of per-user rate, we can see in Fig. 4 that RMMSE+OPA has a 95% probability of having values smaller or equal to 5.5. On the other hand, RMMSE+UPA and MMSE+UPA, have a 95% chance of obtaining values smaller or equal to 4.78 and 4.0, respectively. At last, ZF+OPA has a 95% probability of having values smaller or equal to 5.08. Future work might focus on detection and decoding techniques for cell-free networks [49], [50], [51], [52], [53], [54], [55], [56], [57], [58], [59], [60], [61], [62], [63], [64], [65], [66], [67], [68], [69], [70].

## VI. CONCLUSIONS

In this work, we have developed a novel iterative RMMSE precoder based on generalized loading to mitigate the effects of imperfect CSI in cell-free networks. We devised optimal and uniform power allocation techniques based on the maximization of the minimum SINR, taking the RMMSE precoder into

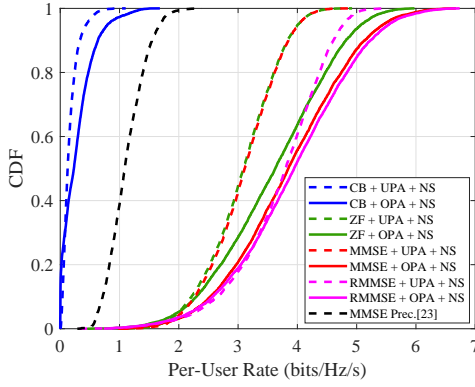


Fig. 4. CDF vs. per-user rate with  $M = 128$ ,  $U = 16$ ,  $n = 0.9$ , 500 channel realizations, SNR = 20 dB and  $E_{tr} = M\rho_f$ .

account. We also performed a sum-rate analysis and evaluated the computational cost of the proposed and existing methods, which shows that the proposed approaches have comparable cost. Numerical results illustrated that the proposed techniques have improved performance in terms of BER, sum-rate and per-user rate in imperfect CSI scenarios.

## REFERENCES

- [1] R. C. de Lamare, "Massive mimo systems: Signal processing challenges and future trends," *URSI Radio Science Bulletin*, vol. 2013, no. 347, pp. 8–20, 2013.
- [2] W. Zhang, H. Ren, C. Pan, M. Chen, R. C. de Lamare, B. Du, and J. Dai, "Large-scale antenna systems with ul/dl hardware mismatch: Achievable rates analysis and calibration," *IEEE Transactions on Communications*, vol. 63, no. 4, pp. 1216–1229, 2015.
- [3] T. L. Marzetta, E. G. Larsson, H. Yang, and H. Q. Ngo, *Fundamentals of Massive MIMO*. Cambridge University Press, nov 2016.
- [4] H. Q. Ngo, A. Ashikhmin, H. Yang, E. G. Larsson, and T. L. Marzetta, "Cell-free massive MIMO versus small cells," *IEEE Transactions on Wireless Communications*, vol. 16, no. 3, pp. 1834–1850, mar 2017.
- [5] L. D. Nguyen, T. Q. Duong, H. Q. Ngo, and K. Tourki, "Energy efficiency in cell-free massive MIMO with zero-forcing precoding design," *IEEE Communications Letters*, vol. 21, no. 8, pp. 1871–1874, aug 2017.
- [6] Q. H. Spencer, A. L. Swindlehurst, and M. Haardt, "Zero-forcing methods for downlink spatial multiplexing in multiuser mimo channels," *IEEE Transactions on Signal Processing*, vol. 52, no. 2, pp. 461–471, 2004.
- [7] V. Stankovic and M. Haardt, "Generalized design of multi-user mimo precoding matrices," *IEEE Transactions on Wireless Communications*, vol. 7, no. 3, pp. 953–961, 2008.
- [8] H. Sung, S. Lee, and I. Lee, "Generalized channel inversion methods for multiuser mimo systems," *IEEE Transactions on Communications*, vol. 57, no. 11, pp. 3489–3499, 2009.
- [9] K. Zu and R. C. de Lamare, "Low-complexity lattice reduction-aided regularized block diagonalization for mu-mimo systems," *IEEE Communications Letters*, vol. 16, no. 6, pp. 925–928, 2012.
- [10] K. Zu, R. C. de Lamare, and M. Haardt, "Generalized design of low-complexity block diagonalization type precoding algorithms for multiuser mimo systems," *IEEE Transactions on Communications*, vol. 61, no. 10, pp. 4232–4242, 2013.
- [11] W. Zhang, R. C. de Lamare, C. Pan, M. Chen, J. Dai, B. Wu, and X. Bao, "Widely linear precoding for large-scale mimo with iqi: Algorithms and performance analysis," *IEEE Transactions on Wireless Communications*, vol. 16, no. 5, pp. 3298–3312, 2017.
- [12] A. R. Flores, R. C. de Lamare, and B. Clerckx, "Linear precoding and stream combining for rate splitting in multiuser mimo systems," *IEEE Communications Letters*, vol. 24, no. 4, pp. 890–894, 2020.
- [13] Y. Cai, R. C. de Lamare, L. Yang, and M. Zhao, "Robust mmse precoding based on switched relaying and side information for multiuser mimo relay systems," *IEEE Transactions on Vehicular Technology*, vol. 64, no. 12, pp. 5677–5687, 2015.
- [14] N. Song, W. U. Alokozai, R. C. de Lamare, and M. Haardt, "Adaptive widely linear reduced-rank beamforming based on joint iterative optimization," *IEEE Signal Processing Letters*, vol. 21, no. 3, pp. 265–269, 2014.
- [15] H. Ruan and R. C. de Lamare, "Robust adaptive beamforming using a low-complexity shrinkage-based mismatch estimation algorithm," *IEEE Signal Processing Letters*, vol. 21, no. 1, pp. 60–64, 2014.
- [16] H. Ruan and R. C. de Lamare, "Robust adaptive beamforming based on low-rank and cross-correlation techniques," *IEEE Transactions on Signal Processing*, vol. 64, no. 15, pp. 3919–3932, 2016.
- [17] H. Ruan and R. C. de Lamare, "Distributed robust beamforming based on low-rank and cross-correlation techniques: Design and analysis," *IEEE Transactions on Signal Processing*, vol. 67, no. 24, pp. 6411–6423, 2019.
- [18] K. Zu, R. C. de Lamare, and M. Haardt, "Multi-branch tomlinson-harashima precoding design for mu-mimo systems: Theory and algorithms," *IEEE Transactions on Communications*, vol. 62, no. 3, pp. 939–951, 2014.
- [19] L. Zhang, Y. Cai, R. C. de Lamare, and M. Zhao, "Robust multibranch tomlinson-harashima precoding design in amplify-and-forward mimo relay systems," *IEEE Transactions on Communications*, vol. 62, no. 10, pp. 3476–3490, 2014.
- [20] A. R. Flores, R. C. De Lamare, and B. Clerckx, "Tomlinson-harashima precoded rate-splitting with stream combiners for mu-mimo systems," *IEEE Transactions on Communications*, pp. 1–1, 2021.
- [21] L. T. N. Landau and R. C. de Lamare, "Branch-and-bound precoding for multiuser mimo systems with 1-bit quantization," *IEEE Wireless Communications Letters*, vol. 6, no. 6, pp. 770–773, 2017.
- [22] J. Gu, R. C. de Lamare, and M. Huemer, "Buffer-aided physical-layer network coding with optimal linear code designs for cooperative networks," *IEEE Transactions on Communications*, vol. 66, no. 6, pp. 2560–2575, 2018.
- [23] Y. Jiang, Y. Zou, H. Guo, T. A. Tsiftsis, M. R. Bhatnagar, R. C. de Lamare, and Y. D. Yao, "Joint power and bandwidth allocation for energy-efficient heterogeneous cellular networks," *IEEE Transactions on Communications*, vol. 67, no. 9, pp. 6168–6178, 2019.
- [24] X. Lu and R. C. de Lamare, "Opportunistic relaying and jamming based on secrecy-rate maximization for multiuser buffer-aided relay systems," *IEEE Transactions on Vehicular Technology*, vol. 69, no. 12, pp. 15 269–15 283, 2020.
- [25] V. M. T. Palhares, A. Flores, and R. C. De Lamare, "Robust mmse precoding and power allocation for cell-free massive mimo systems," *IEEE Transactions on Vehicular Technology*, pp. 1–1, 2021.
- [26] E. Nayebi, A. Ashikhmin, T. L. Marzetta, H. Yang, and B. D. Rao, "Precoding and power optimization in cell-free massive MIMO systems," *IEEE Transactions on Wireless Communications*, vol. 16, no. 7, pp. 4445–4459, jul 2017.
- [27] V. M. Palhares, "Iterative ap selection, mmse precoding and power allocation in cell-free massive mimo systems," *IET Communications*, vol. 14, pp. 3996–4006(10), December 2020. [Online]. Available: <https://digital-library.theiet.org/content/journals/10.1049/iet-com.2020.0627>
- [28] E. Björnson and L. Sanguinetti, "Scalable cell-free massive MIMO systems," *IEEE Transactions on Communications*, vol. 68, no. 7, pp. 4247–4261, jul 2020.
- [29] —, "Making cell-free massive MIMO competitive with MMSE processing and centralized implementation," *IEEE Transactions on Wireless Communications*, vol. 19, no. 1, pp. 77–90, jan 2020.
- [30] G. Interdonato, M. Karlsson, E. Björnson, and E. G. Larsson, "Local partial zero-forcing precoding for cell-free massive MIMO," *IEEE Transactions on Wireless Communications*, vol. 19, no. 7, pp. 4758–4774, jul 2020.
- [31] S. Buzzi, C. D'Andrea, A. Zappone, and C. D'Elia, "User-centric 5G cellular networks: Resource allocation and comparison with the cell-free massive MIMO approach," *IEEE Transactions on Wireless Communications*, vol. 19, no. 2, pp. 1250–1264, feb 2020.
- [32] J. Li, P. Stoica, and Z. Wang, "On robust capon beamforming and diagonal loading," *IEEE Transactions on Signal Processing*, vol. 51, no. 7, pp. 1702–1715, jul 2003.
- [33] A. Elnashar, S. M. Elnoubi, and H. A. El-Mikati, "Further study on robust adaptive beamforming with optimum diagonal loading," *IEEE Transactions on Antennas and Propagation*, vol. 54, no. 12, pp. 3647–3658, dec 2006.
- [34] Y. Cai, R. C. de Lamare, L. Yang, and M. Zhao, "Robust MMSE precoding based on switched relaying and side information for multiuser mimo relay systems," *IEEE Transactions on Vehicular Technology*, vol. 64, no. 12, pp. 5677–5687, dec 2015.
- [35] O. Besson and F. Vincent, "Performance analysis of beamformers using generalized loading of the covariance matrix in the presence of random

- steering vector errors," *IEEE Transactions on Signal Processing*, vol. 53, no. 2, pp. 452–459, feb 2005.
- [36] J. Wang, M. Bengtsson, B. Ottersten, and D. P. Palomar, "Robust MIMO precoding for several classes of channel uncertainty," *IEEE Transactions on Signal Processing*, vol. 61, no. 12, pp. 3056–3070, jun 2013.
- [37] A. Tajer, N. Prasad, and X. Wang, "Robust linear precoder design for multi-cell downlink transmission," *IEEE Transactions on Signal Processing*, vol. 59, no. 1, pp. 235–251, jan 2011.
- [38] C. Shen, T. Chang, K. Wang, Z. Qiu, and C. Chi, "Distributed robust multicell coordinated beamforming with imperfect CSI: An ADMM approach," *IEEE Transactions on Signal Processing*, vol. 60, no. 6, pp. 2988–3003, jun 2012.
- [39] Y. Guo and B. C. Levy, "Worst-case MSE precoder design for imperfectly known MIMO communications channels," *IEEE Transactions on Signal Processing*, vol. 53, no. 8, pp. 2918–2930, aug 2005.
- [40] J. Wang and M. Bengtsson, "Joint optimization of the worst-case robust MMSE MIMO transceiver," *IEEE Signal Processing Letters*, vol. 18, no. 5, pp. 295–298, may 2011.
- [41] H. Shen, J. Wang, W. Xu, Y. Rong, and C. Zhao, "A worst-case robust MMSE transceiver design for nonregenerative MIMO relaying," *IEEE Transactions on Wireless Communications*, vol. 13, no. 2, pp. 695–709, feb 2014.
- [42] H. Ruan and R. C. de Lamare, "Distributed robust beamforming based on low-rank and cross-correlation techniques: Design and analysis," *IEEE Transactions on Signal Processing*, vol. 67, no. 24, pp. 6411–6423, 2019.
- [43] M. Medra and T. N. Davidson, "Low-complexity robust MISO downlink precoder design with per-antenna power constraints," *IEEE Transactions on Signal Processing*, vol. 66, no. 2, pp. 515–527, jan 2018.
- [44] T. Ketseoglou and E. Ayanoglu, "Zero-forcing per-group precoding for robust optimized downlink massive MIMO performance," *IEEE Transactions on Communications*, vol. 67, no. 10, pp. 6816–6828, oct 2019.
- [45] B. Zhang, Z. He, K. Niu, and L. Zhang, "Robust linear beamforming for MIMO relay broadcast channel with limited feedback," *IEEE Signal Processing Letters*, vol. 17, no. 2, pp. 209–212, feb 2010.
- [46] M. Joham, W. Utschick, and J. A. Nossek, "Linear transmit processing in MIMO communications systems," *IEEE Transactions on Signal Processing*, vol. 53, no. 8, pp. 2700–2712, aug 2005.
- [47] S. Boyd and L. Vandenberghe, *Convex Optimization*. Cambridge University Press, 2004.
- [48] A. Tang, J. Sun, and K. Gong, "Mobile propagation loss with a low base station antenna for NLOS street microcells in urban area," in *IEEE VTS 53rd Vehicular Technology Conference, Spring 2001. Proceedings (Cat. No.01CH37202)*. IEEE, may 2001.
- [49] R. C. de Lamare and R. Sampaio-Neto, "Adaptive mber decision feedback multiuser receivers in frequency selective fading channels," *IEEE Communications Letters*, vol. 7, no. 2, pp. 73–75, 2003.
- [50] R. C. De Lamare, R. Sampaio-Neto, and A. Hjorungnes, "Joint iterative interference cancellation and parameter estimation for cdma systems," *IEEE Communications Letters*, vol. 11, no. 12, pp. 916–918, 2007.
- [51] R. C. De Lamare and R. Sampaio-Neto, "Minimum mean-squared error iterative successive parallel arbitrated decision feedback detectors for ds-cdma systems," *IEEE Transactions on Communications*, vol. 56, no. 5, pp. 778–789, 2008.
- [52] Y. Cai and R. C. de Lamare, "Space-time adaptive mmse multiuser decision feedback detectors with multiple-feedback interference cancellation for cdma systems," *IEEE Transactions on Vehicular Technology*, vol. 58, no. 8, pp. 4129–4140, 2009.
- [53] R. C. de Lamare and R. Sampaio-Neto, "Reduced-rank space-time adaptive interference suppression with joint iterative least squares algorithms for spread-spectrum systems," *IEEE Transactions on Vehicular Technology*, vol. 59, no. 3, pp. 1217–1228, 2010.
- [54] Y. Cai and R. C. de Lamare, "Space-time adaptive mmse multiuser decision feedback detectors with multiple-feedback interference cancellation for cdma systems," *IEEE Transactions on Vehicular Technology*, vol. 58, no. 8, pp. 4129–4140, 2009.
- [55] P. Li and R. C. De Lamare, "Adaptive decision-feedback detection with constellation constraints for mimo systems," *IEEE Transactions on Vehicular Technology*, vol. 61, no. 2, pp. 853–859, 2012.
- [56] R. C. de Lamare, "Adaptive and iterative multi-branch mmse decision feedback detection algorithms for multi-antenna systems," *IEEE Transactions on Wireless Communications*, vol. 12, no. 10, pp. 5294–5308, 2013.
- [57] P. Li and R. C. de Lamare, "Distributed iterative detection with reduced message passing for networked mimo cellular systems," *IEEE Transactions on Vehicular Technology*, vol. 63, no. 6, pp. 2947–2954, 2014.
- [58] Y. Cai, R. C. de Lamare, B. Champagne, B. Qin, and M. Zhao, "Adaptive reduced-rank receive processing based on minimum symbol-error-rate criterion for large-scale multiple-antenna systems," *IEEE Transactions on Communications*, vol. 63, no. 11, pp. 4185–4201, 2015.
- [59] R. C. de Lamare and R. Sampaio-Neto, "Adaptive reduced-rank processing based on joint and iterative interpolation, decimation, and filtering," *IEEE Transactions on Signal Processing*, vol. 57, no. 7, pp. 2503–2514, 2009.
- [60] A. G. D. Uchoa, C. T. Healy, and R. C. de Lamare, "Iterative detection and decoding algorithms for mimo systems in block-fading channels using ldpc codes," *IEEE Transactions on Vehicular Technology*, vol. 65, no. 4, pp. 2735–2741, 2016.
- [61] Z. Shao, R. C. de Lamare, and L. T. N. Landau, "Iterative detection and decoding for large-scale multiple-antenna systems with 1-bit adcs," *IEEE Wireless Communications Letters*, vol. 7, no. 3, pp. 476–479, 2018.
- [62] R. B. Di Renna, C. Bockelmann, R. C. de Lamare, and A. Dekorsy, "Detection techniques for massive machine-type communications: Challenges and solutions," *IEEE Access*, vol. 8, pp. 180 928–180 954, 2020.
- [63] R. B. Di Renna and R. C. de Lamare, "Adaptive activity-aware iterative detection for massive machine-type communications," *IEEE Wireless Communications Letters*, vol. 8, no. 6, pp. 1631–1634, 2019.
- [64] —, "Iterative list detection and decoding for massive machine-type communications," *IEEE Transactions on Communications*, vol. 68, no. 10, pp. 6276–6288, 2020.
- [65] —, "Dynamic message scheduling based on activity-aware residual belief propagation for asynchronous mmcs," *IEEE Wireless Communications Letters*, pp. 1–1, 2021.
- [66] F. L. Duarte and R. C. de Lamare, "Cloud-driven multi-way multiple-antenna relay systems: Joint detection, best-user-link selection and analysis," *IEEE Transactions on Communications*, vol. 68, no. 6, pp. 3342–3354, 2020.
- [67] Z. Shao, L. T. N. Landau, and R. C. de Lamare, "Dynamic oversampling for 1-bit adcs in large-scale multiple-antenna systems," *IEEE Transactions on Communications*, pp. 1–1, 2021.
- [68] C. T. Healy and R. C. de Lamare, "Decoder-optimised progressive edge growth algorithms for the design of ldpc codes with low error floors," *IEEE Communications Letters*, vol. 16, no. 6, pp. 889–892, 2012.
- [69] —, "Design of ldpc codes based on multipath emd strategies for progressive edge growth," *IEEE Transactions on Communications*, vol. 64, no. 8, pp. 3208–3219, 2016.
- [70] J. Liu and R. C. de Lamare, "Low-latency reweighted belief propagation decoding for ldpc codes," *IEEE Communications Letters*, vol. 16, no. 10, pp. 1660–1663, 2012.